

ULTRASOUND NEWS

September, 2023

ORIGINAL ARTICLE

Open Access

Evaluation of commercially available point-of-care ultrasound for automated optic nerve sheath measurement

Brad T. Moore^{1*}, Tom Osika¹, Steven Satterly², Shreyansh Shah³, Tim Thirion¹, Spencer Hampton⁴, Stephen Aylward¹ and Sean Montgomery⁵

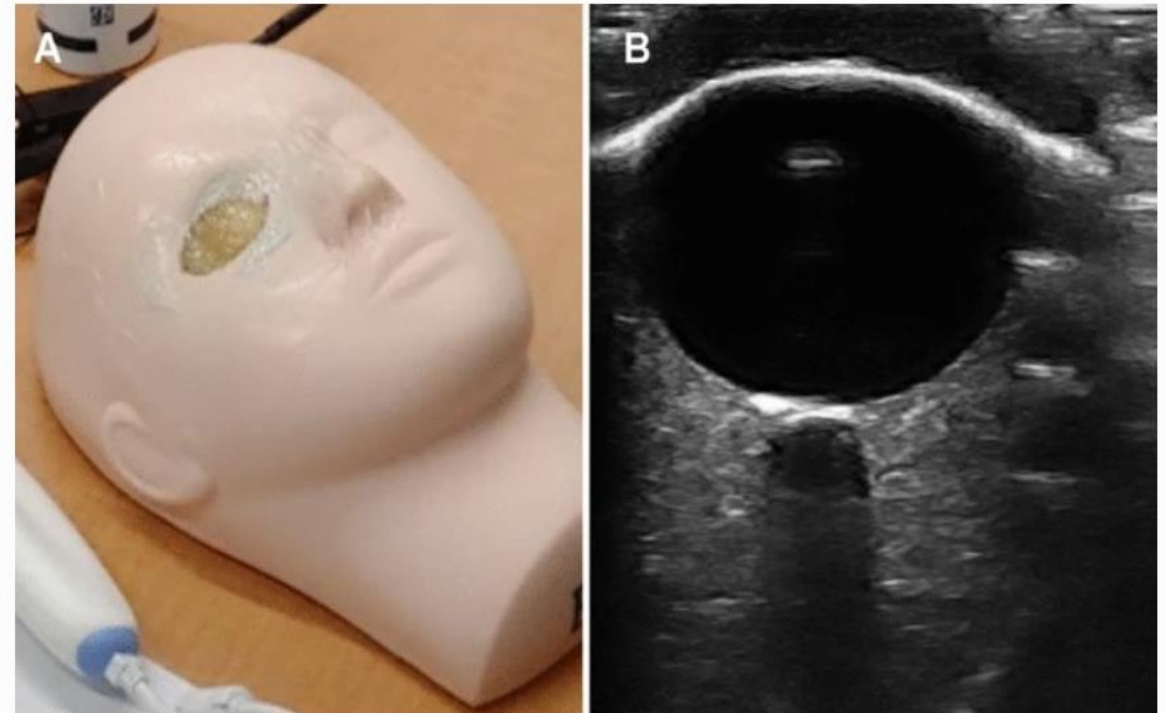
Unskilled operator study

Each participant attended an initial training session followed a week later by the evaluation session. During the training session, participants were described the general anatomy of the ocular orb, the ONS, and the basic principles of ONSD measurement. They were given written instructions for the blind ONSD procedure:

1. Apply ultrasound gel to the eyelid.
2. Place the probe on the center of the eyelid in a horizontal (transverse) orientation
3. Rock the probe to a 30 degree angle upwards
4. Count to eight while slowly moving the probe downwards to an opposing 30 degree angle

Conclusions Ultrasound of the optic nerve sheath has the potential to be a convenient, non-invasive, point-of-injury or triage measure for elevated intracranial pressure in cases of traumatic brain injury. When transducer width is sufficient, briefly trained operators may obtain video sequences of the optic nerve sheath without guidance. This data suggest that unskilled operators are able to achieve the images needed for AI interpretation. However, we also show that image quality differences between ultrasound probes may influence manual ONSD measurements.

Fig. 1



Ocular head phantom. **A.** A picture of the ocular head phantom used in the physician preference and unskilled operator studies. **B.** An example US of the phantom using a Clarius L7HD

REVIEW

Open Access



Ultrasound detected increase in optic disk height to identify elevated intracranial pressure: a systematic review

Ghadi Ghanem^{1*}, David Haase², Agatha Brzezinski², Rikke Ogawa³, Parsa Asachi¹ and Alan Chiem²

Abstract

Background Elevated intracranial pressure (eICP) is a serious medical emergency that requires prompt identification and monitoring. The current gold standards of eICP detection require patient transportation, radiation, and can be invasive. Ocular ultrasound has emerged as a rapid, non-invasive, bedside tool to measure correlates of eICP. This systematic review seeks to explore the utility of ultrasound detected optic disc elevation (ODE) as an ultrasonographic finding of eICP and to study its sensitivity and specificity as a marker of eICP.

Methods This systematic review followed the preferred reporting items for systematic reviews and meta-analyses guidelines. We systematically searched PubMed, EMBASE, and Cochrane Central for English articles published before April 2023; yielding 1,919 total citations. After eliminating duplicates, and screening the records, we identified 29 articles that addressed ultrasonographically detected ODE.

Results The 29 articles included a total of 1249 adult and pediatric participants. In patients with papilledema, the mean ODE ranged between 0.6 mm and 1.2 mm. Proposed cutoff values for ODE ranged between 0.3 mm and 1 mm. The majority of studies reported a sensitivity between 70 and 90%, and specificity ranged from 69 to 100%, with a majority of studies reporting a specificity of 100%.

Conclusions ODE and ultrasonographic characteristics of the optic disc may aid in differentiating papilledema from other conditions. Further research on ODE elevation and its correlation with other ultrasonographic signs is warranted as a means to increase the diagnostic accuracy of ultrasound in the setting of eICP.

Keywords Optic disc elevation, Papilledema, Intracranial pressure, ODE, Optic disc, Point of care ultrasound, Ocular ultrasound, Elevated intracranial pressure, Pseudopapilledema, Ocular ultrasound

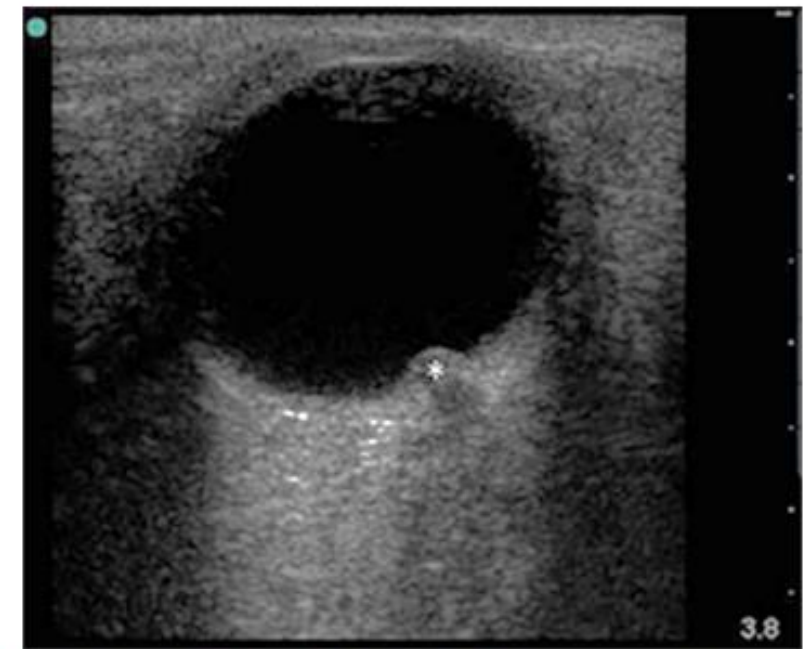


Fig. 1 Elevation of the optic disc, marked with a star on B scan ocular ultrasound

Conclusions

ODE and ultrasonographic characteristics of the optic disc may aid in differentiating papilledema from other ocular conditions. Furthermore, ODE has the potential to be used in conjunction with ONS diameter as a correlate of eICP. Larger, prospective studies are needed to assess the role of ODE elevation and its correlation with other ultrasonographic signs, such as ONS diameter, the crescent sign and the 30-degree test in patients with suspected eICP.



Restricted access | Research article | First published online December 23, 2022

Cross-sectional area and echo intensity values of peripheral nerves: Ultrasonographic and cadaveric correlation

[Mohini Rawat](#)  , [Vanessa M Reddin](#) , [...], and [Chirag Upreti](#)  [View all authors and affiliations](#)

[Volume 31, Issue 3](#) | <https://doi.org/10.1177/1742271X221139199>

ABSTRACT

INTRODUCTION:

ULTRASONOGRAPHY ALLOWS HIGH-RESOLUTION VISUALISATION OF THE PERIPHERAL NERVES FOR QUANTITATIVE AND QUALITATIVE ANALYSES. WE REPORT CROSS-SECTIONAL AREA VALUES (QUANTITATIVE MEASURE) AND ECHO INTENSITY VALUES (QUALITATIVE MEASURE) FOR 46 PERIPHERAL NERVE SITES IN UPPER AND LOWER EXTREMITIES IN CADAVERIC SPECIMENS.

OBJECTIVE:

TO DETERMINE CROSS-SECTIONAL AREA VALUES AND ECHO INTENSITY VALUES OF PERIPHERAL NERVES OF UPPER AND LOWER EXTREMITIES AT 46 NERVE SITES.

METHODS:

NERVE MEASUREMENTS WERE OBTAINED USING ELECTRONIC CALLIPERS AND ULTRASONOGRAPHY FOR LINEAR DIMENSION AND CROSS-SECTIONAL AREA MEASUREMENTS, RESPECTIVELY, IN SIX CADAVERIC SPECIMENS FOR 46 PERIPHERAL NERVE SITES. ULTRASOUND IMAGES WERE FURTHER ANALYSED TO ESTIMATE ECHO INTENSITY PERCENTAGE VALUES FOR 46 NERVES.

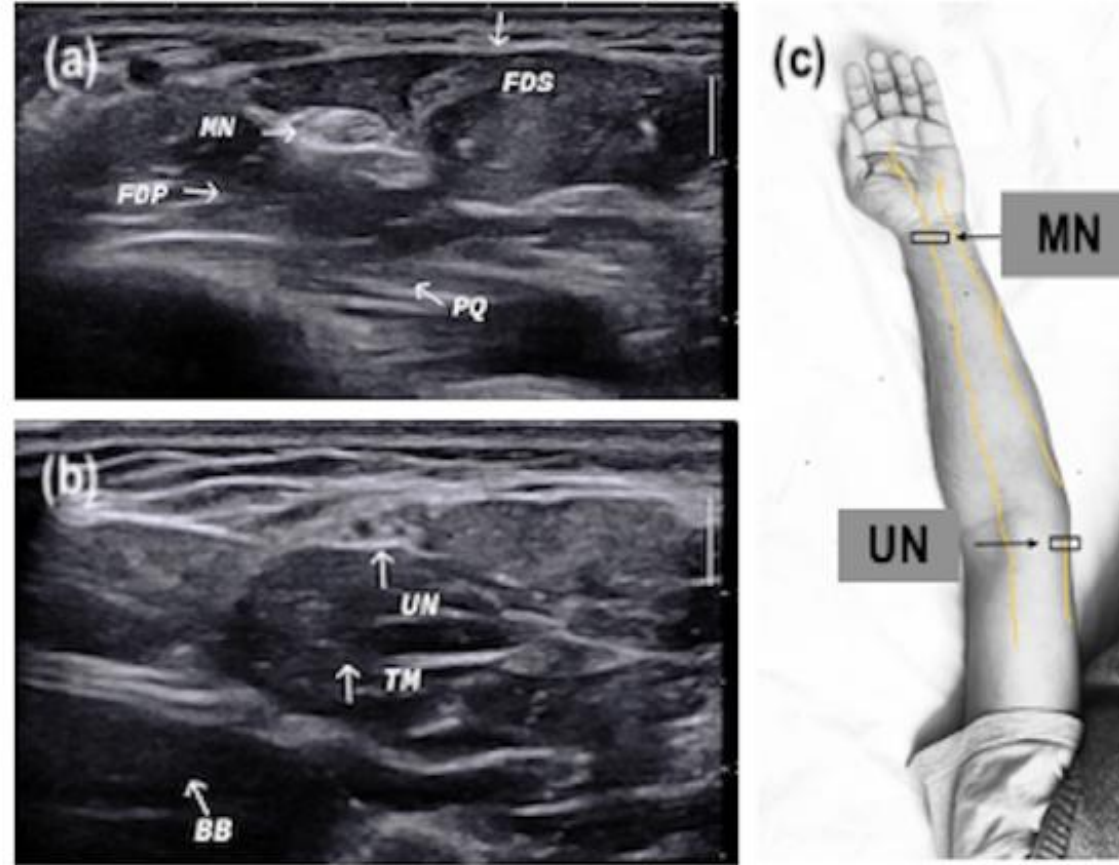
RESULTS:

WE PRESENT NORMAL CROSS-SECTIONAL AREA VALUES OF VARIOUS NERVES OF UPPER AND LOWER EXTREMITIES WITH THEIR RESPECTIVE ECHO INTENSITY VALUES. CALCULATED CROSS-SECTIONAL AREA VALUES FROM LINEAR DIMENSIONS DID NOT MATCH THE MEASURED CROSS-SECTIONAL AREA VALUES VIA TRACE METHOD.

CONCLUSION:

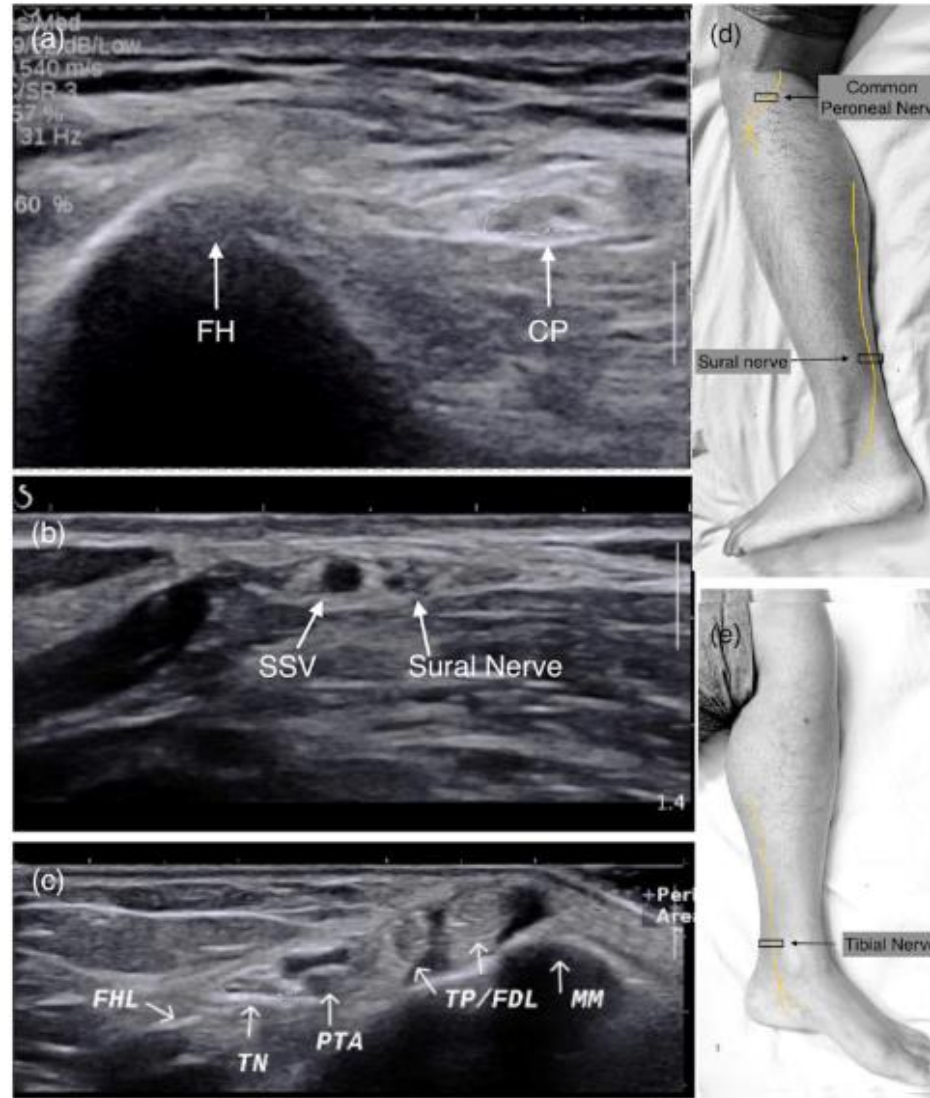
CROSS-SECTIONAL AREA VALUES (QUANTITATIVE MEASURE) AND ECHO INTENSITY VALUES (QUALITATIVE MEASURE) FOR 46 PERIPHERAL NERVE SITES IN UPPER AND LOWER EXTREMITIES IN CADAVERIC SPECIMENS ARE PRESENTED. THE ESTIMATION OF CROSS-

Figure 1.



Transverse ultrasound section of median and ulnar nerves (marked with white arrows) at different locations with anatomical landmarks. (a) MN distal forearm between FDS and FDP at the level of PQ proximal end. (b) UN distal arm next to medial head of TM and nearby BB muscle. (c) Image showing course of nerve with probe position (black box). BB, biceps brachii; FDP, forearm deep digital flexor; FDS, forearm superficial digital flexor; MN, median nerve; PQ, pronator quadratus; TM, triceps muscle; UN, ulnar nerve

Figure 2.



Transverse ultrasound section of common peroneal, sural and tibial nerves (marked with white arrows) at different locations with anatomical landmarks. (a) CP nerve near the FH. (b) Sural nerve distal leg adjacent to SSV. (c) TN at ankle (MM, TP/FDL, PTA and veins, FHL tendon). (d, e) Image showing course of nerve with probe position (black box). CP, common peroneal; FDL, flexor tendons; FH, fibular head; FHL, flexor hallucis longus; MM, medial malleolus; PTA, posterior tibial artery; SSV, short saphenous vein; TN, tibial nerve.



[J Ultrason](#). 2022 Oct; 22(91): e209–e215.

Published online 2022 Oct 1. doi: [10.15557/jou.2022.0035](https://doi.org/10.15557/jou.2022.0035)

PMCID: PMC9714279

PMID: [36483783](https://pubmed.ncbi.nlm.nih.gov/36483783/)

Role of High-resolution Ultrasonography in the Evaluation of the Tibial and Median Nerves in Diabetic Peripheral Neuropathy

[Tanu Ranjan](#), ¹ [Shruti Chandak](#),^{✉1,*} [Ankur Malhotra](#), ¹ [Arijit Aggarwal](#), ¹ [Jigar Haria](#), ¹ and [Deepak Singla](#) ¹

► [Author information](#) ► [Article notes](#) ► [Copyright and License information](#) [PMC Disclaimer](#)

Abstract

[Go to:](#) ►

Aim

To evaluate and measure the mean cross-sectional area of the tibial and median nerves in patients with diabetic peripheral neuropathy, and to study the association between high-resolution ultrasonographic findings in diabetic peripheral neuropathy with the duration of illness, glycosylated haemoglobin values, random blood sugar levels, and aesthesiometry (using monofilament examination).

Material and methods

A prospective observational study was conducted among 63 patients who were diagnosed with type 2 diabetes mellitus and underwent ultrasound and monofilament examinations. The cross-sectional area of the median nerve of the dominant hand and the tibial nerves was calculated on ultrasound examination.

In our study, the cross-sectional area of the tibial and median nerves was found to correlate strongly with HbA_{1c} levels, RBS levels, duration of diabetes, and monofilament examination. In our opinion, HRU in combination with HbA_{1c} levels and monofilament examination can be regarded as an easily available, inexpensive, and effective technique for detecting changes secondary to peripheral neuropathy.

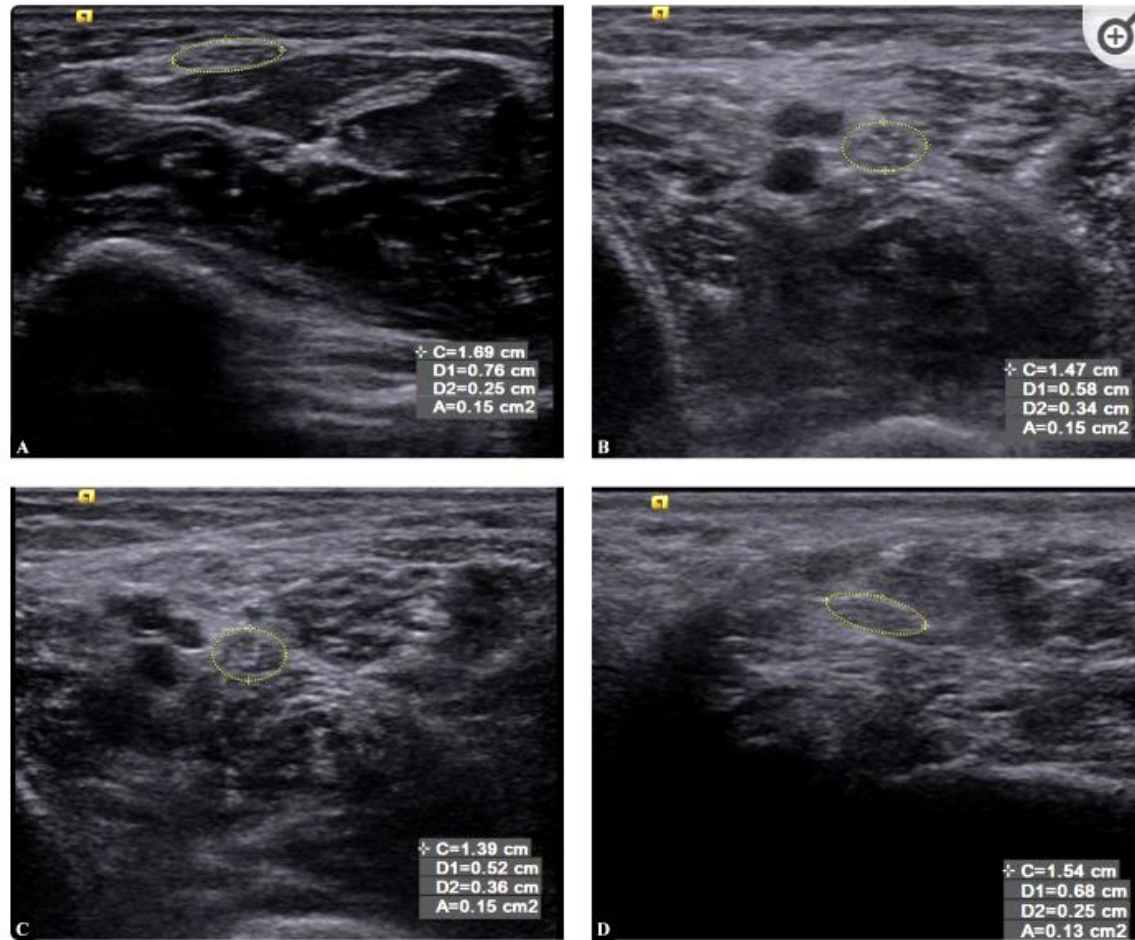


[Fig. 1.](#)

Transverse grey-scale ultrasound showing: **A.** Thickening of median nerve in a 65-year-old male patient diagnosed with T2DM 10 years previously. The patient had pain in both lower limbs. His HbA_{1c} was 9% and his random blood sugar value was 400 mg/dl. It shows mean cross-sectional area of 15 mm². **B.** Thickening of tibial nerve at 1 cm proximal to medial malleolus (in the same patient). **C.** Thickening of tibial nerve (in the same patient) at 3 cm proximal to medial malleolus. **D.** Thickening of tibial nerve (in the same patient) at 5 cm proximal to medial malleolus

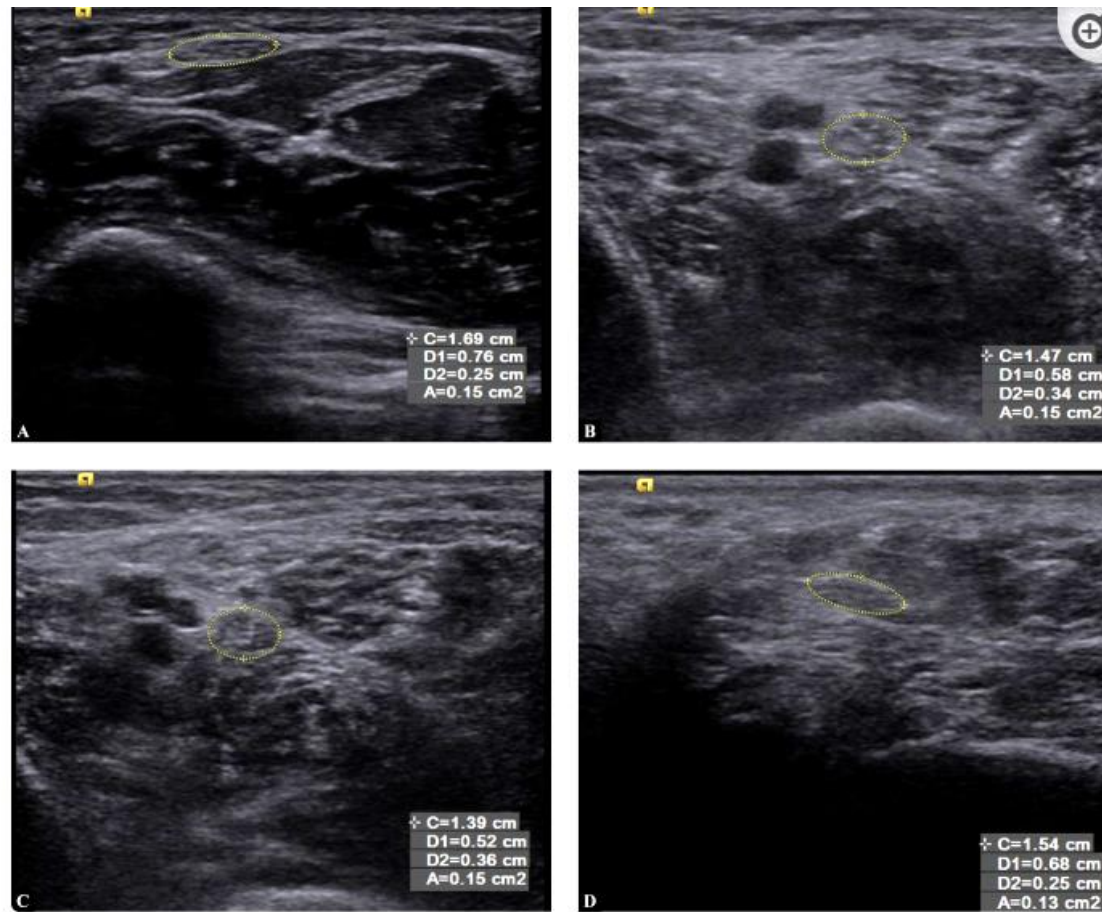


[Fig. 1.](#)

Transverse grey-scale ultrasound showing: **A.** Thickening of median nerve in a 65-year-old male patient diagnosed with T2DM 10 years previously. The patient had pain in both lower limbs. His HbA_{1c} was 9% and his random blood sugar value was 400 mg/dl. It shows mean cross-sectional area of 15 mm². **B.** Thickening of tibial nerve at 1 cm proximal to medial malleolus (in the same patient). **C.** Thickening of tibial nerve (in the same patient) at 3 cm proximal to medial malleolus. **D.** Thickening of tibial nerve (in the same patient) at 5 cm proximal to medial malleolus



Nerve entrapment syndromes: detection by ultrasound

Christoph Schwabl¹, Gernot Schmidle², Peter Kaiser², Elena Drakonaki³, Mihra S. Taljanovic⁴, Andrea S. Klauser¹

¹Radiology Department, Medical University Innsbruck, Innsbruck, Austria; ²Department for Orthopedics and Traumatology, Medical University Innsbruck, Innsbruck, Austria;

³Independent MSK Radiology Practice, Heraklion, Greece; ⁴Department of Medical Imaging, Banner University Medical Center, The University of Arizona, College of Medicine, Tucson, AZ, USA

Nerve entrapment syndromes are commonly encountered in clinical practice. Accurate diagnosis and management require a knowledge of peripheral neuroanatomy and the recognition of key clinical symptoms and findings. Nerve entrapment syndromes are frequently associated with structural abnormalities of the affected nerve. Therefore, imaging allows the evaluation of the cause, severity, and etiology of the entrapment. High-resolution ultrasonography can depict early and chronic morphological changes within the entire nerve course and is therefore an ideal modality for diagnosing various nerve entrapment syndromes in different regions. This review article presents some of the most common types of nerve entrapment, with special focus on ultrasound imaging and key findings.

Keywords: Entrapment neuropathy; Median nerve; Carpal tunnel syndrome; Ultrasonography; Ulnar nerve

Key points: High-resolution ultrasonography is a feasible, fast, and reliable method to diagnose nerve entrapment syndromes. Ultrasound findings include enlargement of the nerve at the site of compression, hourglass narrowing, loss of the echotexture, and echogenic perineural fibrosis. Anatomical landmarks and morphological features are key for understanding and identifying nerve entrapments on ultrasonography.

ULTRA SONO GRAPHY

REVIEW ARTICLE

<https://doi.org/10.14366/usg.22186>
eISSN: 2288-5943

Ultrasonography 2023;42:376-387

Received: November 11, 2022
Revised: January 17, 2023
Accepted: February 2, 2023

Correspondence to:

Christoph Schwabl, MD, Radiology Department, Medical University Innsbruck, Anichstrasse 35, A-6020 Innsbruck, Austria

Tel. +4351250483950

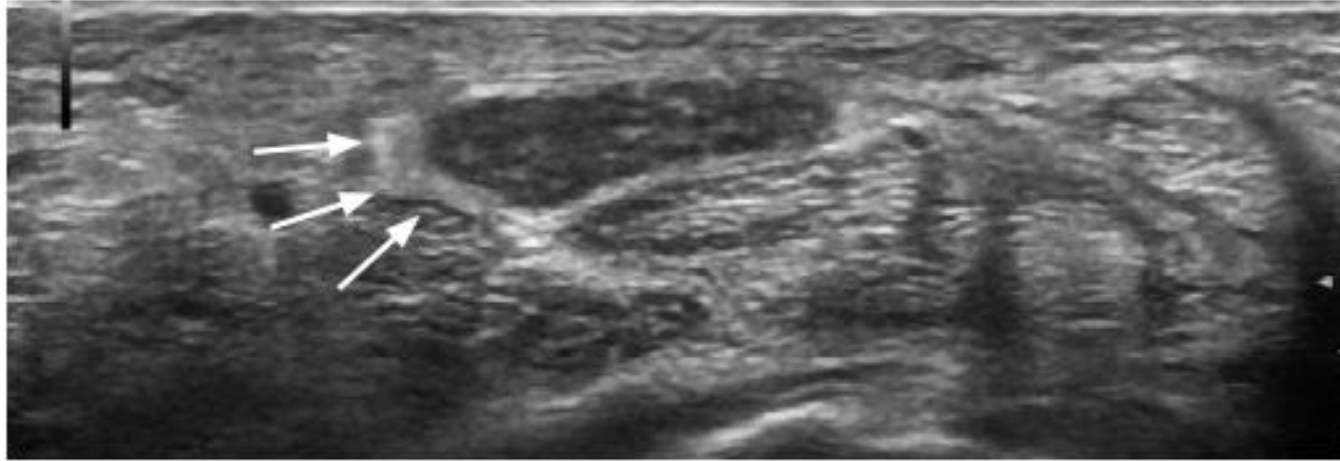
Fax. +4351250422758

E-mail: Christoph.schwabl@i-med.ac.at

This is an Open Access article distributed under the terms of the Creative Commons Attribution Non-Commercial License (<http://creativecommons.org/licenses/by-nc/4.0/>) which permits unrestricted non-commercial use, distribution, and reproduction in any medium, provided the original work is properly cited.

Conclusion

High-resolution US is a feasible, fast, and reliable method to diagnose and monitor nerve entrapment syndromes and to guide diagnostic and therapeutic perineural injections. US findings include enlargement of the diameter and CSA of the nerve at the site of compression, hourglass narrowing in the longitudinal section, the loss of echotexture, echogenic perineural fibrosis, decreased mobility, and intraneural fibrosis in longstanding entrapment conditions.



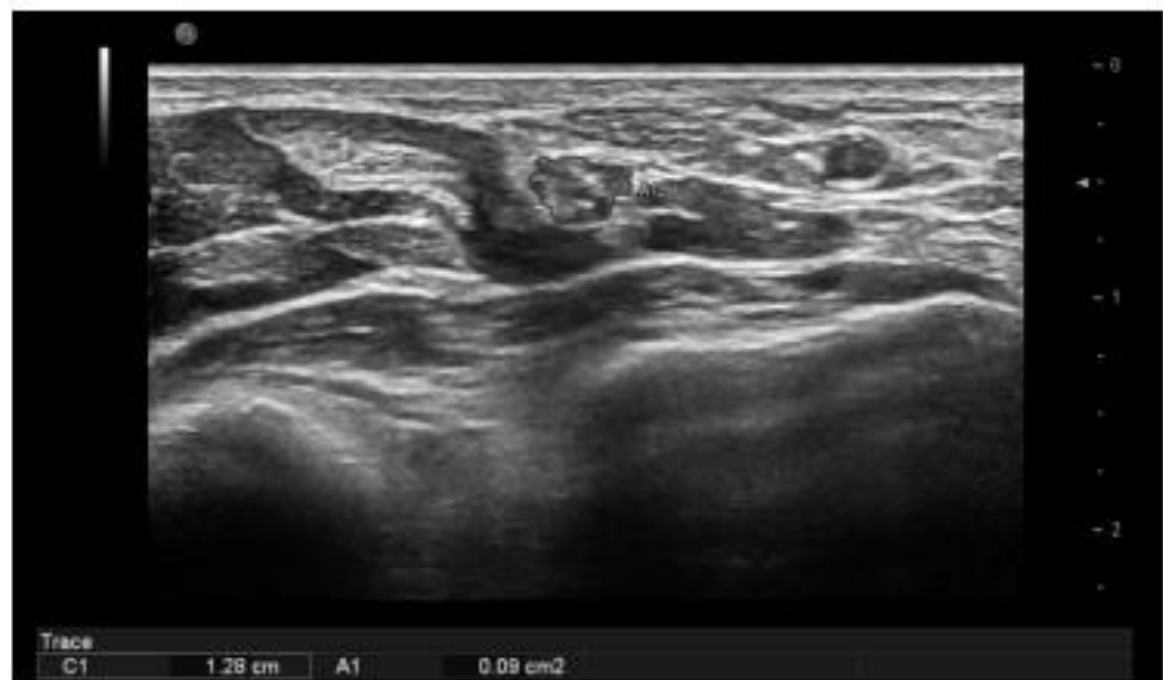
A



B

Fig. 1. A 78-year-old patient with unilateral symptoms of carpal tunnel syndrome.

A. The ultrasonography examination reveals a swollen, hypoechoic nerve with a thickened perineurium on the affected side (arrows). **B.** The other hand shows a normal median nerve inside the carpal tunnel with a typical honeycomb-like appearance, with hypoechoic nerve fascicles and hyperechoic interfascicular perineurium (arrows).



A



B

Fig. 2. A 56-year-old patient with the clinical presentation of carpal tunnel syndrome.

On ultrasonography, the cross-sectional area of the median nerve at the level of the pronator quadratus (A) and within the carpal tunnel (B) shows a pathological delta value of 12 mm². The nerve has a blurred echotexture and is hypoechoic and swollen.

Nerve entrapments

ULTRASONOGRAPHY

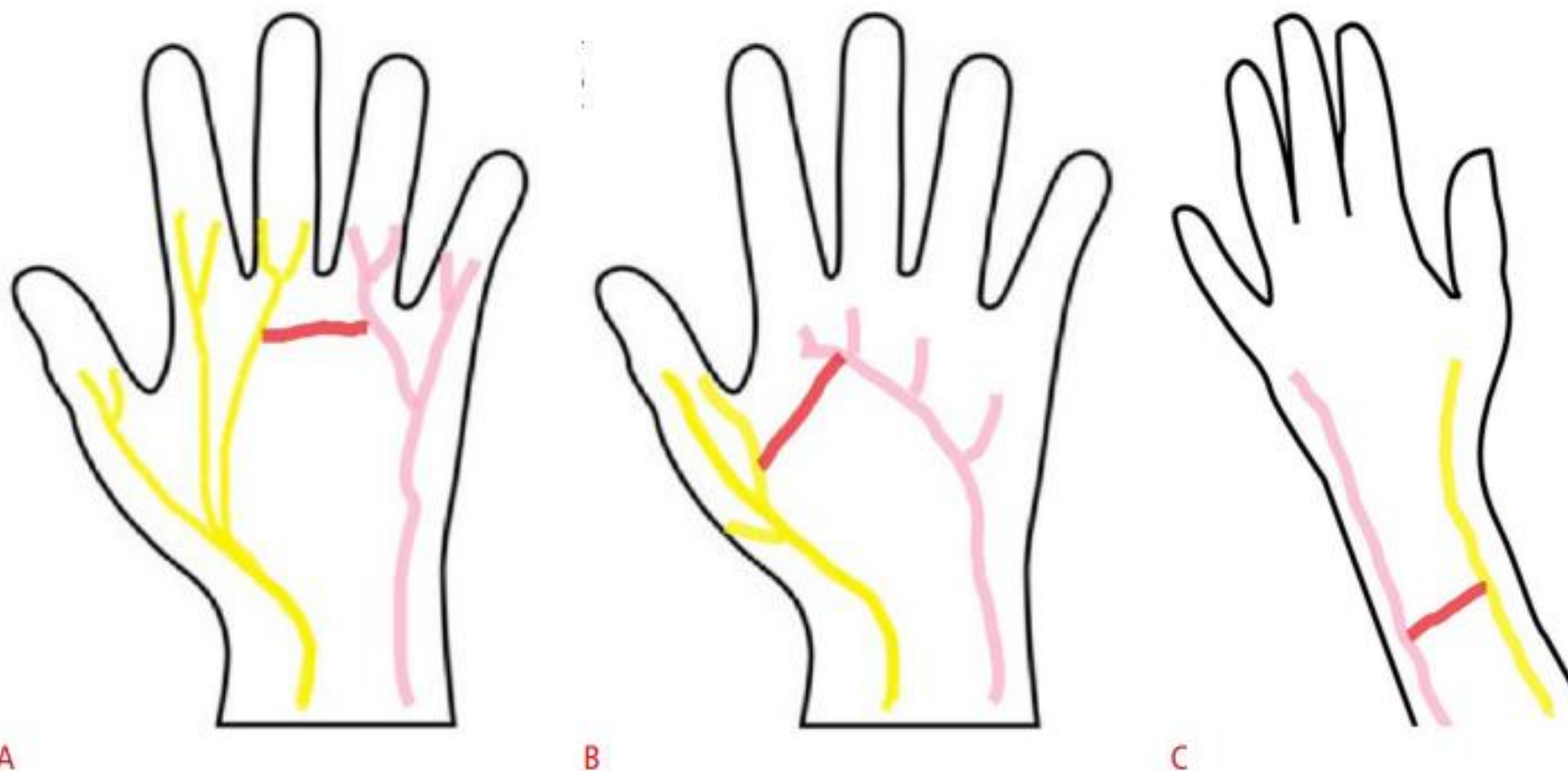
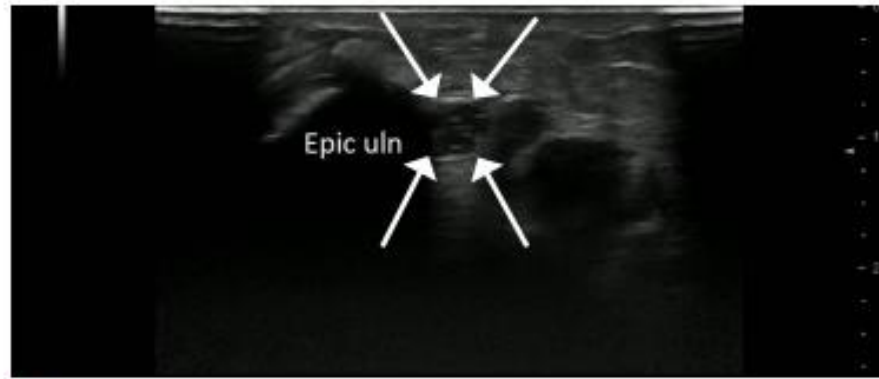
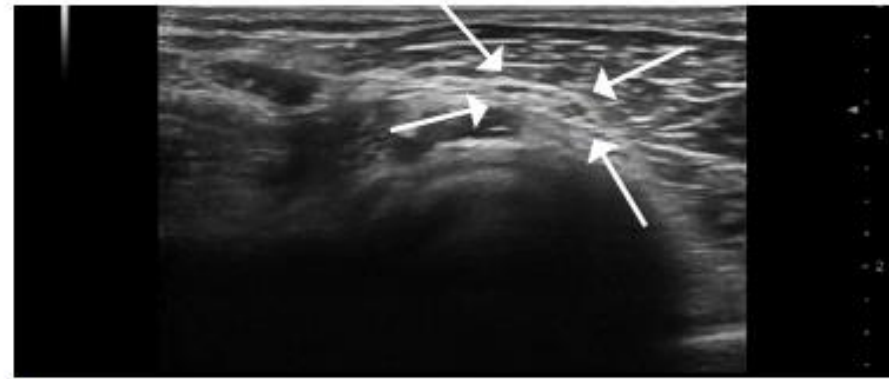


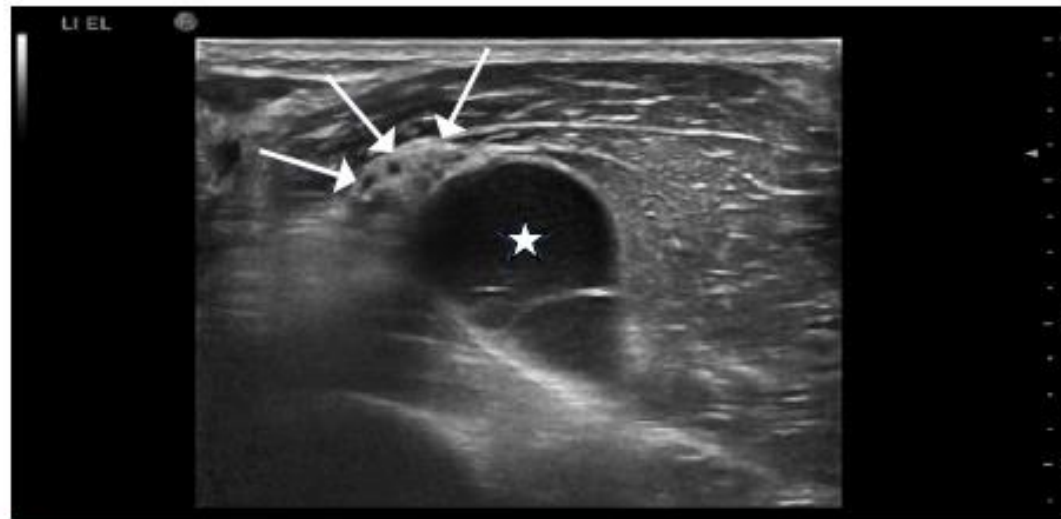
Fig. 3. Schematic diagrams of Berrettini anastomosis (A), Riche-Cannieu anastomosis (B), and Martin-Gruber anastomosis (C).



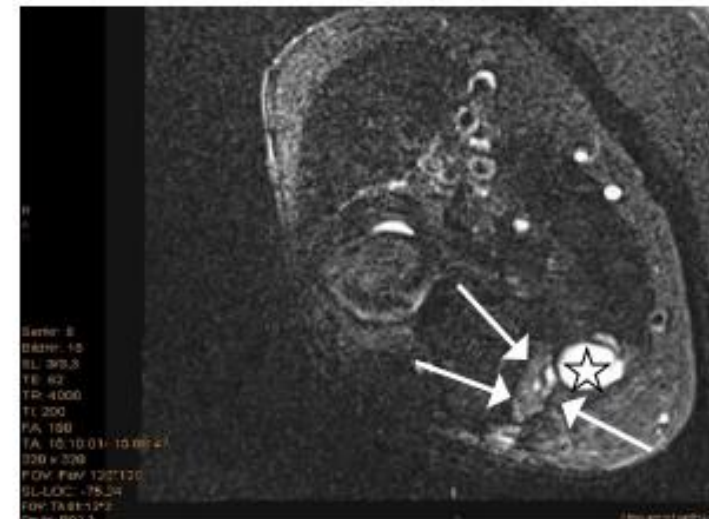
A



B



C



D

Fig. 5. A 53-year-old patient presenting with persistent cubital tunnel syndrome.

A, B. Ultrasonography examination shows a hypoechoic, swollen ulnar nerve, within the cubital tunnel (**A**) with echogenic perineurium (**B**) (arrows). **C.** A large septated joint ganglion (star) with displacement of the nerve (arrows) in the cubital tunnel can be visualized adjacent to the nerve. **D.** T2-weighted axial magnetic resonance imaging with fat saturation shows the ganglion (star) and the swollen hyperintense nerve (arrows) with a better overview of the region.

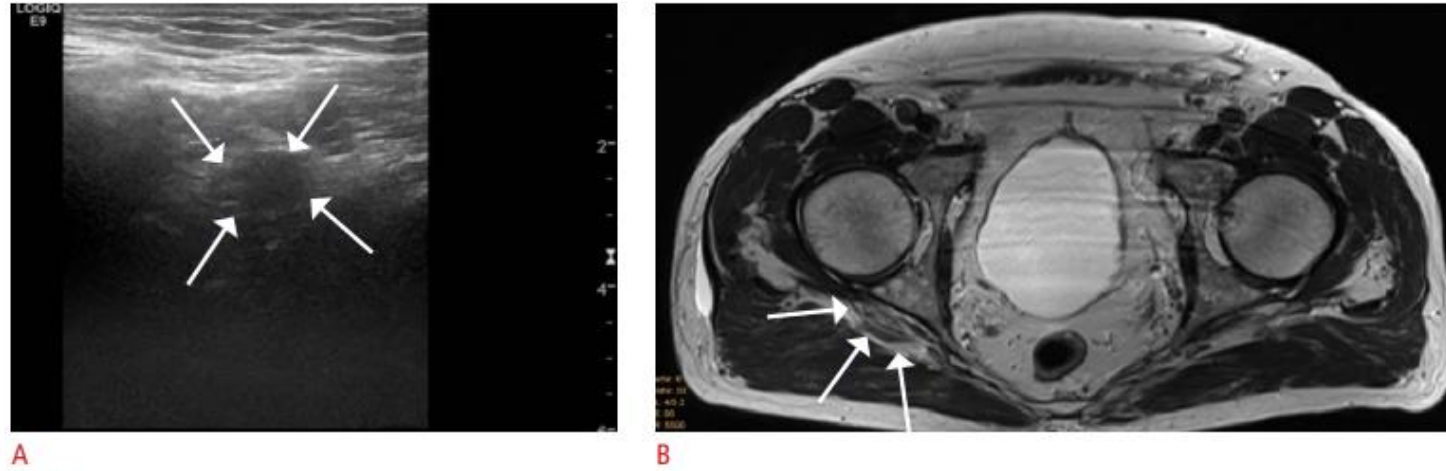


Fig. 7. A 67-year-old patient presenting with sciatica, who underwent previous magnetic resonance imaging of the spine to rule out affection of the nerve roots.
A, B. On ultrasonography (A), the sciatic nerve (arrows) appears hypoechoic and swollen, with corresponding changes of the nerve on T2-weighted magnetic resonance imaging (B).

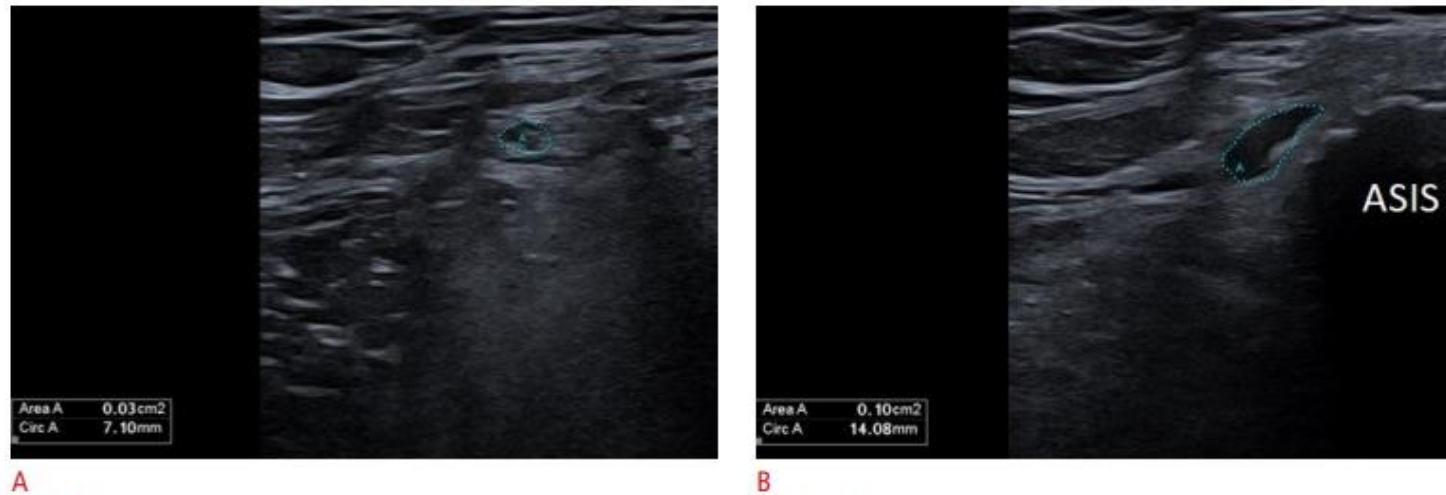


Fig. 8. A 41-year-old patient presenting with numbness and pain in the lateral thigh.
A, B. On ultrasonography, the lateral cutaneous femoris nerve is seen to be hypoechoic and swollen at the level of the anterior superior iliac spine (ASIS) with an increased cross-sectional area.

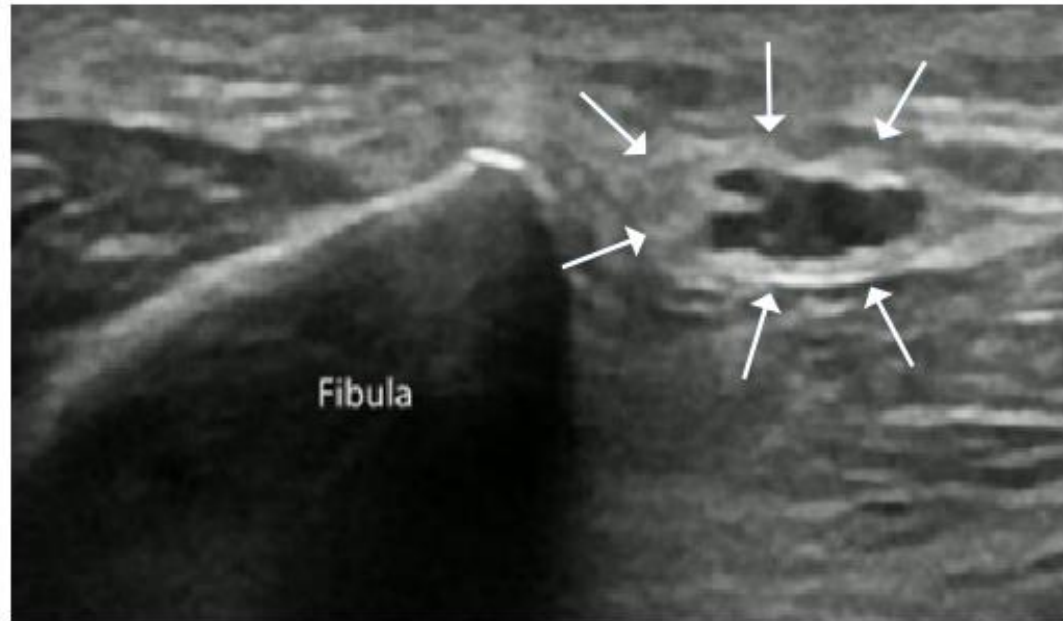


Fig. 9. A 60-year-old patient presenting with foot drop and numbness in the lower extremity. On a ultrasonography examination, the common peroneal nerve (arrows) at the level of the fibular head shows swollen fascicles and a thickened perineurium.

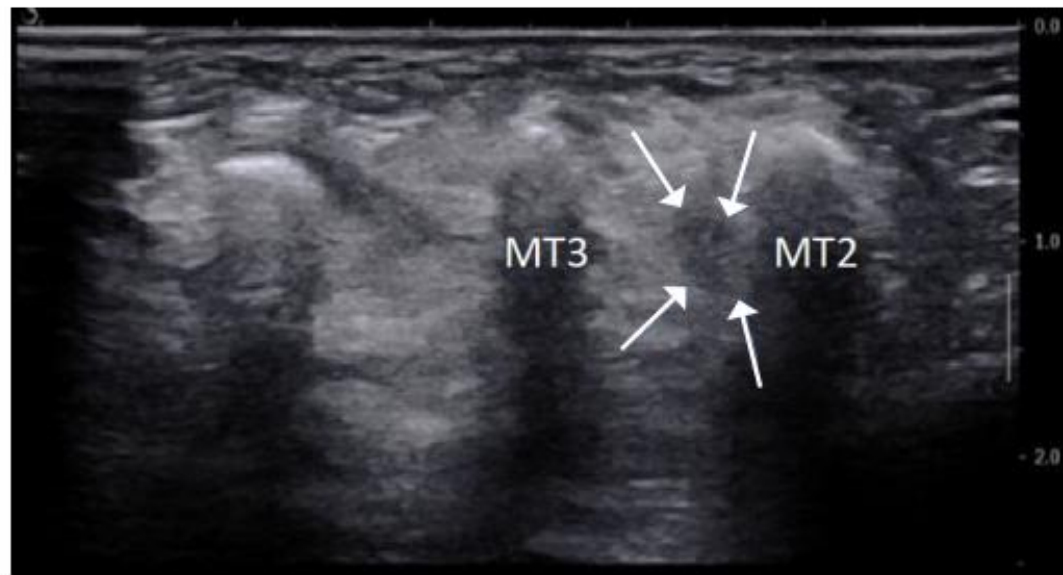


Fig. 10. A 63-year-old patient with electrifying pain while walking between metatarsal (MT) 2 and 3. On ultrasonography, a hypoechoic Morton's neuroma (arrows) between the heads of MT 2 and 3 is visible.

Characteristics of the static muscle stiffness of ankle plantar flexors in individuals with chronic ankle instability

Takumi Kobayashi, Taiki Kodesho ... Keigo Taniguchi

Original Article—Orthopedics | Published: 28 August 2023



Purpose

Individuals with chronic ankle instability (CAI) have deficits in closed kinetic chain dorsiflexion that may perpetuate injury. Determining the characteristics of muscle stiffness in the plantar flexors of individuals with CAI may help in developing appropriate treatments. We aimed to highlight the characteristics of static muscle stiffness in ankle plantar flexor muscles during the passive dorsiflexion of the ankle joint in individuals with CAI.

Methods

A total of 30 patients were included in the study based on the International Ankle Consortium criteria. The patients were categorized evenly into healthy, coper, and CAI groups (i.e., 10 patients in each group). After measuring the dorsiflexion range of motion (non-weight-bearing/weight-bearing) of the ankle joint, the static muscle stiffness measurements of the medial gastrocnemius, lateral gastrocnemius, soleus, and peroneus longus were obtained. The measurements were performed during the knee joint's extension and 50° flexion and passive dorsiflexion between the range of 40° plantar flexion and 20° dorsiflexion.

Abstract

Results

The dorsiflexion range of motion of the CAI group was significantly smaller than that of the healthy and coper groups in the weight-bearing position. No interaction was observed for muscle stiffness in both the knee flexion and extension positions, and no significant differences were identified among the three groups.

The shear modulus of the soleus at 20° ankle dorsiflexion with knee flexion had a significant negative correlation with the weight-bearing range of motion of the ankle.

Conclusion

The limitation in the weight-bearing dorsiflexion range of motion in CAI was largely due to factors other than the increased elasticity of the ankle plantar flexor muscles.